



## Effect of hydration on the dielectric properties of C-S-H gel

Silvina Cerveny, Silvia Arrese-Igor, Jorge S. Dolado, Juan J. Gaitero, Angel Alegría et al.

Citation: *J. Chem. Phys.* **134**, 034509 (2011); doi: 10.1063/1.3521481

View online: <http://dx.doi.org/10.1063/1.3521481>

View Table of Contents: <http://jcp.aip.org/resource/1/JCPSA6/v134/i3>

Published by the [American Institute of Physics](http://www.aip.org).

---

### Related Articles

Spatio-temporal behaviors of a clock reaction in an open gel reactor  
*Chaos* **16**, 037109 (2006)

Magnetic resonance imaging of chemical waves in porous media  
*Chaos* **16**, 037103 (2006)

Gaussian random field models of aerogels  
*J. Appl. Phys.* **93**, 4584 (2003)

Germinating surfaces in reaction-diffusion systems? Experiments and a hypothesis  
*J. Chem. Phys.* **117**, 6646 (2002)

Electronic confinement of organic molecules in confined spaces: A spectroscopic study of Zn(phen)<sub>2</sub>(NO<sub>3</sub>)<sub>2</sub> loaded MCM-41  
*J. Chem. Phys.* **117**, 5959 (2002)

---

### Additional information on *J. Chem. Phys.*

Journal Homepage: <http://jcp.aip.org/>

Journal Information: [http://jcp.aip.org/about/about\\_the\\_journal](http://jcp.aip.org/about/about_the_journal)

Top downloads: [http://jcp.aip.org/features/most\\_downloaded](http://jcp.aip.org/features/most_downloaded)

Information for Authors: <http://jcp.aip.org/authors>

### ADVERTISEMENT



**AIP Advances**

*Submit Now*

**Explore AIP's new  
open-access journal**

- **Article-level metrics  
now available**
- **Join the conversation!  
Rate & comment on articles**

## Effect of hydration on the dielectric properties of C-S-H gel

Silvina Cerveny,<sup>1,a)</sup> Silvia Arrese-Igor,<sup>1</sup> Jorge S. Dolado,<sup>2</sup> Juan J. Gaitero,<sup>2</sup> Angel Alegría,<sup>1,3</sup> and Juan Colmenero<sup>1,3,4</sup>

<sup>1</sup>Centro de Física de Materiales (CSIC, UPV/EHU)-Materials Physics Center, Paseo Manuel de Lardizabal 5, 20018, San Sebastián, Spain

<sup>2</sup>LABEIN-Tecnalia, Parque tecnologico de Bizkaia 48160-Derio, Spain

<sup>3</sup>Departamento de Física de Materiales, UPV/EHU, Facultad de Química, 20018, San Sebastián, Spain

<sup>4</sup>Donostia International Physics Center, San Sebastián, Spain

(Received 28 June 2010; accepted 8 November 2010; published online 20 January 2011)

The behavior of water dynamics confined in hydrated calcium silicate hydrate (C-S-H) gel has been investigated using broadband dielectric spectroscopy (BDS;  $10^{-2}$ – $10^6$  Hz) in the low-temperature range (110–250 K). Different water contents in C-S-H gel were explored (from 6 to 15 wt%) where water remains amorphous for all the studied temperatures. Three relaxation processes were found by BDS (labeled 1 to 3 from the fastest to the slowest), two of them reported here for the first time. We show that a strong change in the dielectric relaxation of C-S-H gel occurs with increasing hydration, especially at a hydration level in which a monolayer of water around the basic units of cement materials is predicted by different structural models. Below this hydration level both processes 2 and 3 have an Arrhenius temperature dependence. However, at higher hydration level, a non-Arrhenius behavior temperature dependence for process 3 over the whole accessible temperature range and, a crossover from low-temperature Arrhenius to high-temperature non-Arrhenius behavior for process 2 are observed. Characteristics of these processes will be discussed in this work. © 2011 American Institute of Physics. [doi:10.1063/1.3521481]

### I. INTRODUCTION

Cements are one of the most used and most valuable materials in the world.<sup>1,2</sup> When water is added to the cement grains, a myriad of chemical reaction takes place to produce a solid skeleton called cement paste that evolves over time. This cement paste can be viewed as a composite in which calcium hydroxide (portlandite) crystals, aluminates, and nonreacted cement powders are embedded into an amorphous nanostructured hydration product, the so-called calcium silicate hydrate (C-S-H) gel.<sup>3</sup> From all the constituents, the major and most important one is precisely the C-S-H gel, since most of the properties of cementitious materials crucially depend on it. The C-S-H gel (the main component of white cement and ordinary Portland cement) has a variable stoichiometry with a general formula  $C_xSH_y$ , where C=CaO, S=SiO<sub>2</sub>, H=H<sub>2</sub>O (this notation is commonly used by the cement chemistry community). Its water content ( $\nu$ ) clearly depends on the specific relative humidity conditions, and therefore on the drying or wetting state. The calcium to silicon ratio (C/S= $x$ ) can range from 1.2 to 2.1, though most of the studies<sup>3–5</sup> report values consistent with a C/S = 1.7.

Although the actual structure of C-S-H has not been fully resolved yet, several microstructural models have been proposed in the past to describe the structure of C-S-H gel as well as the formation of gel and capillary pores. The early work of Powers and Brownyard<sup>6–8</sup> proposed that the C-S-H gel is composed of particles that have a layered structure arranged randomly and bonded together by surface forces as

in clays. Later Feldman and Sereda<sup>9</sup> improved this model by considering that the sheets composing the C-S-H gel do not have an ordered layered structure but they are rather an irregular array of single layers in which water molecules are structurally incorporated in the C-S-H structure. These surfaces are covered by hydroxyl groups which are able to establish hydrogen bonds with the surrounding water molecules. In fact, Sereda<sup>10</sup> in 1980 classified the water contained in cement pastes into three types: (1) *chemically bound water* (also called nonevaporable), is chemically bound to cement particles and becomes part of the cement gel; (2) *physically bound water* (also called chemisorbed water) occupies the gel pores; and (3) *free water* is water inside the capillary pores. We have to note that a similar water classification has been also used for other complex systems such as proteins or deoxyribonucleic acid (DNA).<sup>11</sup> Finally, we put special emphasis on the most recent colloidal model (CM) proposed by Jennigs,<sup>5,12,13</sup> since it can explain most of the experimental results reported in the literature regarding to hydrated cement. According to this model, the basic unit of C-S-H is a colloidal particle (globules) having a size of about 4 nm with a layered internal structure [in agreement with other models in the literature (see Refs. 14–18, and 19)]. During hydration, these globules form clusters to produce a porous structure with two different characteristic lengths: small gel pores (dimensions 1–3 nm) and large gel pores (dimensions 3–12 nm). Consequently, during the cure reaction water can be located in different confinement lengths ranging from 1 to 12 nm. Although, small-angle neutron scattering (SANS) measurements are consistent with particles of ~4 nm C-S-H features,<sup>5</sup> the existence of the globules in C-S-H gel is not experimentally probed. In this sense

<sup>a)</sup> Author to whom correspondence should be addressed. Electronic mail: scerveny@ehu.es.

recently,<sup>20</sup> x-ray scattering measurements with synchrotron x rays on synthetic C-S-H seem to reveal a nanocrystalline order with a particle diameter in the range of 3.5 nm. Regardless of the model considered, the structure of C-S-H gel is highly complex and comprises pores of different sizes in which water molecules can be located. To probe the state of water in C-S-H gel, diverse experimental techniques were used in the literature such as nuclear magnetic resonance (NMR)<sup>21–23</sup> and neutron scattering (NS).<sup>23–25</sup> In particular, analysis of hydrated C-S-H gel by <sup>1</sup>H (proton) NMR time, which is sensitive to water dynamics, has shown three components of hydration water in cement pastes (free water, water adsorbed into hydration products, and located within hydrates), in agreement with most of the structural models. In addition, and also to analyze the distribution of water molecules in this complex material, several researchers<sup>26–30</sup> have studied the dielectric response of cement-based materials mainly in the high-frequency range (10<sup>4</sup>–10<sup>9</sup> Hz) but also in the low-frequency range<sup>31</sup> (10<sup>–2</sup>–10<sup>6</sup> Hz) at room temperatures or higher. However, to our knowledge, dielectric studies at sub-zero temperatures are missing in the literature.

On the other hand, the dynamics of water in confined geometries is one of the great challenges that has always fascinated the scientific community due to its significant repercussion in several fields of biological, chemical, and physical sciences. From this point of view, it is relevant to know how water dynamics is modified by the presence of different environments. In particular, the dynamics of supercooled confined water is one of the hot topics in the physics of condensed matter as revealed by several publications, contradictory results, and the lack of a coherent frame in the last years.<sup>32–35</sup>

In this work, we have analyzed the hydration level dependence of water dynamics in hydrated C-S-H gel by means of broadband dielectric spectroscopy (BDS) at low temperatures (110 to 250 K). This technique is appropriate for the study of water dynamics mainly due to its sensitivity to the high dipolar moment of water molecules. As we will show in this contribution, increasing water content has significant consequences on the supercooled water dynamics in this system. We found a deep change in the water dynamics, especially when crossing the concentration where one water monolayer covers the surface of C-S-H gel.

## II. EXPERIMENTAL

C-S-H samples were prepared by hydration of pure tricalcium silicate (C<sub>3</sub>S). Sample preparation consisted of mixing 5 g of C<sub>3</sub>S with 1400 g of distilled water. The great water to C<sub>3</sub>S ratio used served to maintain calcium concentration in the solution low enough to prevent portlandite precipitation, but without affecting the formation of the C-S-H gel. In addition, water had been previously boiled and the resulting dispersion was sealed in a container to avoid carbonation. After 39 days of continuous stirring at room temperature, the dispersion was filtered and the obtained solid was dried in an oven at 60 °C for an hour. The resulting C-S-H gel had a water content (*c<sub>w</sub>*, expressed as grams of water/grams of dry cement) of *c<sub>w</sub>* = 28 wt. %.

TABLE I. Activation energy *E<sub>a</sub>* and pre-exponential factor (log (τ<sub>0</sub>[s])) corresponding to process 2 and 3 for data in Figs. 5 and 6.

Sample	<i>c<sub>w</sub></i> [wt. %]	Process 2		Process 3	
		log (τ <sub>0</sub> [s])	<i>E<sub>a</sub></i> [eV]	log (τ <sub>0</sub> [s])	<i>E<sub>a</sub></i> [eV]
CSH-06	6.25	– 16.9 ± 0.1	0.37 ± 0.02	–13.2 ± 0.1	0.52 ± 0.02
CSH-09	9.75	–17.3 ± 0.1	0.39 ± 0.02	–13.6 ± 0.1	0.54 ± 0.02
CSH-11	11.00	–16.5 ± 0.4	0.39 ± 0.02	–15.1 ± 0.2	0.54 ± 0.02
CSH-15	15.10	–17.0 ± 0.2	0.43 ± 0.02	–	–

Immediately after, different hydration levels were reached by drying the samples at 100 °C in a vacuum oven. This temperature allows water evaporation without structural damage. In Table I, final water content determined by both thermogravimetry measurements and directly weighting the samples is shown. The samples were labeled as CSH-06, CSH-09, CSH-11, and CSH-15, indicating the water content.

Broadband dielectric spectroscopy is a technique based on the interaction of an external field with the electric dipole moment of the sample.<sup>36–38</sup> With this technique it is possible to study the molecular dynamics in a broad frequency (10<sup>–6</sup> to 10<sup>+11</sup> Hz) and temperature range. The fluctuations of local electrical fields are measured and they can be connected to the dynamics on a molecular scale. To perform a dielectric measurement, the sample is placed between two metallic electrodes which form a capacitor. For parallel-plate configuration, the sample capacitance is expressed as  $C = \epsilon d/A$ , where  $\epsilon$  is the dielectric permittivity of the sample,  $A$  is the sample surface area, and  $d$  its thickness. The material properties are characterized by the complex dielectric permittivity,  $\epsilon^*$ , which is defined as  $\epsilon^*(\omega) = C^*(\omega)/C_0 = \epsilon'(\omega) - i \epsilon''(\omega)$ , where  $C_0$  is the capacitance of the free space.

A broadband dielectric spectrometer, Novocontrol Alpha analyzer, was used to measure the complex dielectric function,  $\epsilon^*(\omega) = \epsilon'(\omega) - i \epsilon''(\omega)$ ,  $\omega = 2\pi f$ , in the frequency ( $f$ ) range from  $f = 10^{-2}$  Hz to  $f = 10^6$  Hz. The samples were placed between parallel gold-plated electrodes with a diameter of 30 mm and the thickness was about 0.4 mm. Isothermal frequency scans recording  $\epsilon^*(\omega)$  were performed every 5 degrees over the temperature range 110–300 K. Sample temperature was controlled by a nitrogen gas flow with stability better than ± 0.1 K. In addition, the sample CSH-06 was further dried directly in the dielectric cell cryostat at 120 °C for 1.5 h and measured again with the same protocol as the samples above.

Standard calorimetric measurements [differential scanning calorimetry (DSC)] were performed by means of a Q2000TA Instrument using cooling and heating rates of 10 K/min. Hermetic aluminum pans were used for all the materials. The sample weights were about 10 mg.

Finally, thermogravimetric analysis was done by using a TGA-Q500 (TA Instruments). All the measurements were conducted under high-purity nitrogen flow over a temperature range of 30–800 °C with a ramp rate of 10 K/min.

## III. RESULTS

Water behavior inside the structure of C-S-H gel was first characterized by DSC. No crystallization at all (on cooling

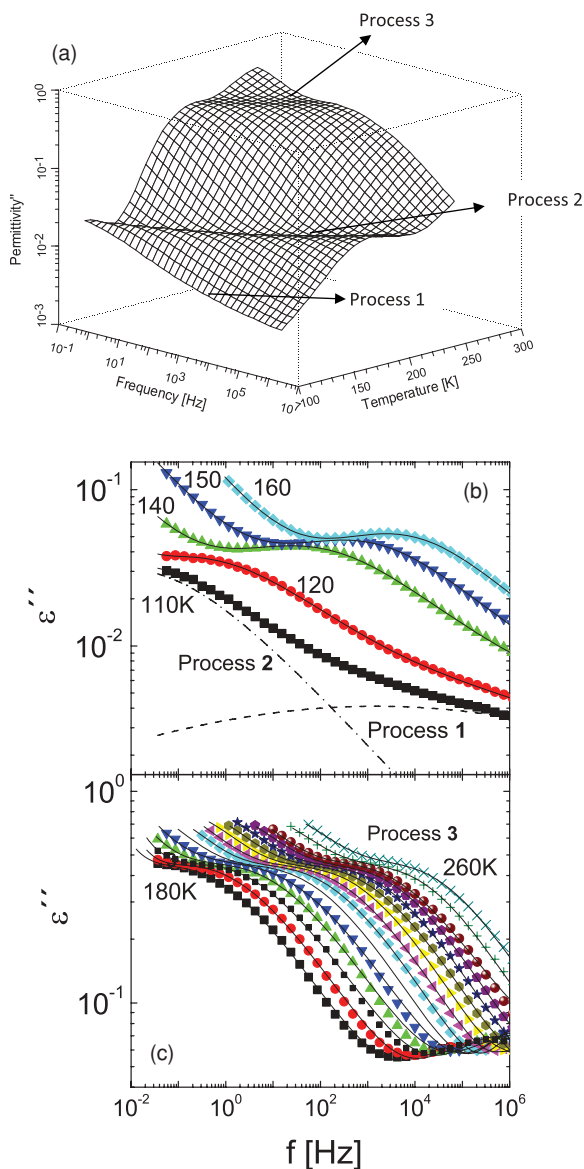


FIG. 1. (a) Three-dimensional plot of the frequency and temperature dependence of the dielectric permittivity  $\epsilon''(\omega)$  for the sample CSH-11. Two processes (2 and 3) are clearly observed on the dielectric spectra for the different temperatures. (b) Dielectric loss spectra of CSH-11 measured at different temperatures (110, 120, 140, 150, and 160 K); (c) Dielectric loss spectra of CSH-11 measured at temperatures from 180 K to 260 K each 5 K. Process 1, 2, and 3 denotes the three dielectric processes observed. The solid line through the data points represents the fits to the experimental data. In (b) dotted line represents the relaxation corresponding to process 1 whereas the dashed-dotted line represents process 2.

or heating) is observed for all the samples analyzed in this work and therefore water remains amorphous in the whole temperature range analyzed. Repeated cooling/heating scans up to a temperature of 100 °C gave reproducible DSC signals indicating that the structure of C-S-H gel was not damaged by either freezing at 110 K or heating up to 373 K. In addition, although samples with water concentration higher than 15 wt. % will not be analyzed in this work, we mention that already at 17 wt. % a small exothermic peak on cooling is observed in the calorimetric measurements, indicating water crystallization from this water content.

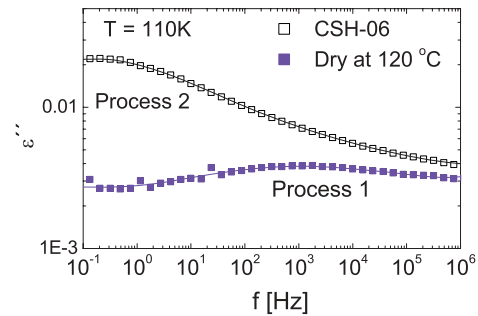


FIG. 2. Dielectric loss spectra at a fixed temperature (110 K) of CSH-06 (open symbols) and the sample further dried at 120 °C (full symbols). Process 2 vanishes by drying at 120 °C whereas process 1 remains in the dielectric spectra.

Figure 1(a) shows a three-dimensional plot of the frequency and temperature dependence of the dielectric permittivity  $\epsilon''(\omega)$  for the sample CSH-11. In addition, the same set of data is also represented as function of frequency at different temperatures [Fig. 1(b): 110 to 160 K and Fig. 1(c): 170 to 250 K]. Although only two processes are clearly seen in Fig. 1(a), we have noticed that to fit the loss spectra at low temperatures [(Fig. 1(b)) we needed an extra process at high frequencies. This process is only slightly resolved in the dielectric spectra since the more prominent process 2 masks its presence. By drying the samples at higher temperature (120 °C) most of the water molecules can be evaporated. This further drying allows resolving unequivocally process 1. Figure 2 shows the comparison between the dielectric loss for sample CSH-06 and the same sample dried at 120 °C during 1.5 h. After drying, process 1 is clearly resolved in the dielectric window and its relaxation times can be well evaluated. As we will see below, we can take advantage of this observation when fitting the dielectric spectra at different water concentrations. Therefore, we conclude that the dielectric response of C-S-H gel has to be decomposed in three dielectric relaxation processes (labeled from the faster process 1 to the slower process 3).

Since all the dielectric processes in C-S-H gel are symmetric, to fit the imaginary part of the dielectric permittivity at the different temperatures and water concentrations we have used the superposition of three Cole–Cole (CC) functions,<sup>39</sup>

$$\epsilon^*(\omega) = \epsilon_\infty + \sum_{j=1}^3 \frac{\Delta\epsilon_j}{[1 + (i\omega\tau_j)^{\alpha_j}] - i\frac{\sigma}{\epsilon_0\omega^s}}, \quad (1)$$

each one related with the three processes observed in Figs. 1(a)–1(c). In Eq. (1)  $\sigma/\omega^s$  is a generalized conductivity contribution,  $\alpha_j$  is the shape parameter that determines the symmetric broadening of the relaxation peak ( $0 < \alpha \leq 1$ ),  $\Delta\epsilon_j = \epsilon_s - \epsilon_\infty$ , is the relaxation strength,  $\epsilon_\infty$  and  $\epsilon_s$  are the unrelaxed and relaxed values of the dielectric constant,  $\tau_j$  is a characteristic relaxation time, and  $\omega$  is the angular frequency. However, as mentioned above, process 1 is masked by the high-frequency flank of process 2 and therefore the relaxation times corresponding to this process are difficult to determine by a completely free fitting procedure. To overcome this problem, the relaxation times corresponding to process 1 were fixed to those obtained from the data analysis of the sample

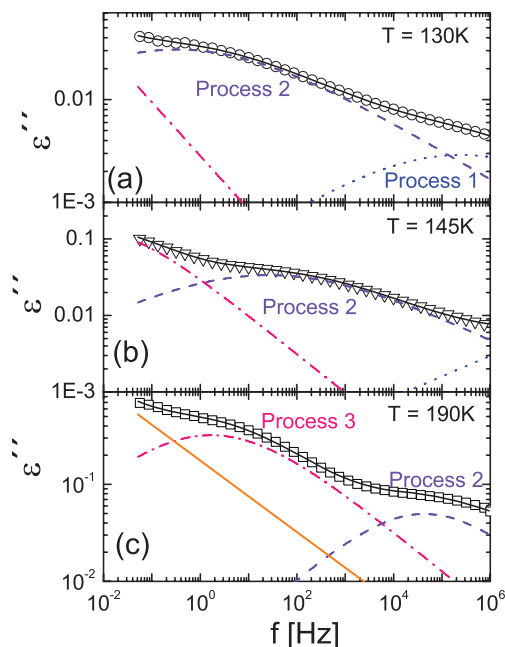


FIG. 3. Frequency-dependent losses of the complex dielectric permittivity,  $\varepsilon''(f)$ , of the sample CSH-15 at three different temperatures 130 K (a), 145 K (b), and 195 K (c). The solid line through the data points is a least-square fit to a superposition of the imaginary part of three Cole–Cole functions for processes 1, 2, and 3 (see text). Dotted, dashed, and dashed-dotted lines represent the relaxation corresponding to process 1, 2, and 3, respectively.

dried at 120 °C (shown in Fig. 2). Thus the overall dielectric spectra were described by Eq. (1), where all the parameters were free except  $\tau_1$  which was fixed as explained above. Figures 3(a)–3(c) show an example of this fitting procedure for the sample CSH-15 at three different temperatures [ $T = 130, 145,$  and  $190$  K in Figs. 3(a)–3(c), respectively].

The relaxation strength ( $\Delta\varepsilon$ ) corresponding to each of these processes [see Eq. (1)] is temperature independent but obviously affected by the amount of water. In Figs. 4(a) and 4(b) average values of  $\Delta\varepsilon_i$  were plotted as a function of  $c_w$ . In all the cases, a clear increase with water content is observed. In Fig. 4(b), the value of  $\Delta\varepsilon_1$  for the sample dried at 120 °C is also included. This sample is taken as a reference and thereby assigned to  $c_w \approx 0$  wt. %. In addition, processes 2 and 3 from this sample cannot be detected and therefore we also set  $\Delta\varepsilon_2$  and  $\Delta\varepsilon_3 = 0$  when  $c_w \approx 0$  wt. %.

The temperature dependence of the relaxation times for the different samples and processes are shown in Figs. 5(a)–5(d). The relaxation times follow different behaviors depending on the water content of the samples. At water concentration lower than 10 wt. % all the processes (1 to 3) follow an Arrhenius behavior in the whole temperature range analyzed. However, at water concentration of 11.0 wt. %, process 2 slightly departs from the Arrhenius behavior at a temperature about 140 K [see Fig. 5(c)]. Moreover, at a higher water concentration (15 wt. %), process 3 is evidently non-Arrhenius whereas process 2 presents a clear crossover from high- $T$  non-Arrhenius to low- $T$  Arrhenius behavior at a temperature of  $T_{\text{cross}} = 145$  K. In the range where the relaxation times show an Arrhenius-like temperature dependence [ $\tau = \tau_0 \exp(E_a/kT)$ ], the activation energies,  $E_a$ , and  $\log(\tau_0)$

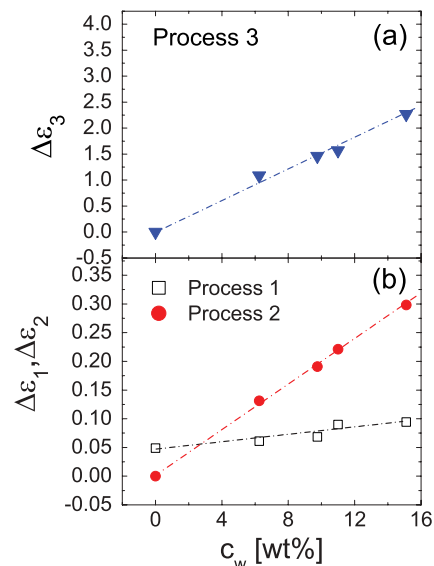


FIG. 4. (a) Average dielectric strength [ $\Delta\varepsilon_3$  in (a) and  $\Delta\varepsilon_1, \Delta\varepsilon_2$  in (b)] for processes 1 to 3 observed in C-S-H gel as a function of water content. The dielectric strength increases with water concentration, indicating that water molecules are involved in all the dielectric processes observed. In (b) the point at  $c_w = 0$  wt. % represents the relaxation strength for process 1 of the sample dried at 120 °C (although some water content different from zero is expected for this sample).

were calculated. Both values are shown in Table I for processes 2 and 3, respectively. For process 1 (not included in the table), the activation energy is  $E_a = 0.20$  eV and  $\log(\tau_0) = -13.00$  s.

Finally, Fig. 6 shows the comparison of the relaxation time for the slowest process 3 [Fig. 6(a)] and the intermediate process 2 [Fig. 6(b)] for the different water content. Note that although both processes 2 and 3 seem to be originated by

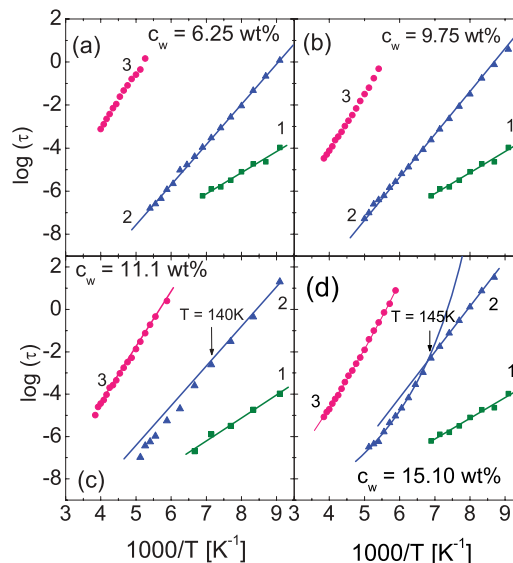


FIG. 5. Temperature dependence of the relaxation time  $\tau(T)$  for C-S-H samples analyzed in this work. All three processes (1 to 3) have an Arrhenius temperature dependence at low water content [see (a) and (b)]. In (d) process 2 shows a slight crossover at 145 K whereas process 3 has Vogel–Fulcher–Tamman temperature dependence. The lines are fits according to the Arrhenius or VFT equation (see text).

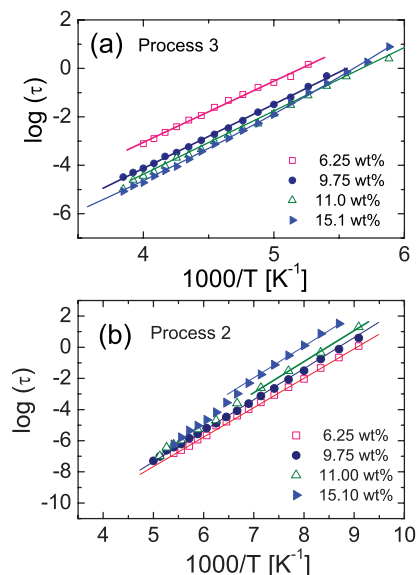


FIG. 6. Comparison of the temperature dependence of the relaxation time  $\tau(T)$  for process 3 [in (a)] and process 2 [in (b)] at the different water contents analyzed in this work.

water molecules (as  $\Delta\epsilon$  increases in a linear way with water content, see Fig. 3) process 3 becomes faster with increasing water concentration, whereas process 2 becomes slower with increasing hydration level. This disparate behavior (between process 2 and 3 with hydration level) indicates that each process is originated from water molecules in different environments of the samples.

#### IV. DISCUSSION

As mentioned in the Introduction, the precise structure of C-S-H is still under debate. However, most of the current models represent C-S-H gel as made of tiny solid particles with water trapped in the nanopore network. The surface of these pores of variable size is covered by hydroxyl groups coming from both silanol (SiOH) and Ca(OH) groups. In addition to the surfaces, and due to the nature of C-S-H gel, nanometric interparticle holes are pools where water can be located. The size and shape of both particles and channels where water can be located varies from 1 to 100 nm. In a recent study<sup>40</sup> on cement pastes by means of DSC and near-infrared spectroscopy, two main populations of water molecules were found. Water molecules were predominantly located in the small gel pores (1–3 nm) whereas a lesser quantity was located in the large gel pores<sup>40</sup> (3–12 nm). Although the water content analyzed in Ref. 40 is higher than in our case (because our water content is lower than the threshold of crystallization), both systems are rather similar.

The fact that the dielectric strength of the processes observed in hydrated C-S-H gel increases with water concentration evidences that they are related with the water dipole reorientation. In addition, activation energies corresponding to processes 2 and 3 are consistent with the corresponding water processes in other systems such as water in hard or soft confinement.<sup>41–46</sup> Moreover, by further drying the samples at 120 °C, processes 2 and 3 vanish from the dielec-

tric spectra, indicating that the origin of these processes is water, which can be evaporated at high temperatures. On the contrary, process 1 remains in the dielectric spectra although its intensity diminishes. By additional drying (up to 300 °C, data not shown in this paper), the relaxation strength further falls but this process still remains in the dielectric spectra. This fact suggests that the origin of process 1 can be related with some molecular movement of the C-S-H itself (likely OH groups) coupled with water molecules since its dielectric strength increases with increasing water concentration. Therefore this relaxation corresponds to the fluctuation of Si(OH) or Ca(OH) groups on the surface of C-S-H gel affected by water molecules.<sup>47</sup> However, more studies are necessary to probe this hypothesis and therefore this process will not be discussed further in the present paper.

Summarizing, we can conclude that water molecules are involved in all the dielectric processes observed in C-S-H gel. Our results are also supported in part by other works in the literature<sup>49–51</sup> that overlap in temperature/frequency with process 3 (note that processes 1 and 2 were not previously reported). With this picture in mind, in the following we will only discuss the water related processes 2 and 3 observed in C-S-H gel at different hydration levels reached by progressively dehydrating the samples.

#### A. Water dynamics at low hydration level ( $c_w < 10$ wt. %)

As mentioned above, the temperature dependence of the relaxation times corresponding to processes 2 and 3 at low water content ( $c_w \leq 10$  wt. %) follows an Arrhenius behavior over the entire temperature range [see Figs. 5(a) and 5(b)]. It should be noted that the formation of one water monolayer on the pore walls is detected by means of adsorption curves during dehydration<sup>8,52</sup> at a water content of about 10 wt. %. Consequently we can conclude that when less than one monolayer of water is present on the surface of gel C-S-H, the dielectric processes 2 and 3 both show an Arrhenius temperature dependence.

The observation of an Arrhenius behavior at low hydration levels is in agreement with that observed in water solutions of other hydrophilic systems at  $c_w < 30$  wt. % (solutions of synthetic polymers) and  $c_w < 20$  wt. % (sugars- or low molecular weight glass formers–water solutions).<sup>41,48,53</sup> At these low water concentrations, few hydrogen bonds are established by water molecules (i.e., no tetrahedrally hydrogen bound water molecules or big water clusters exist) and the relaxation times show Arrhenius behavior over the entire temperature range. Additionally, the relaxation spectra corresponding to processes 2 and 3 are also broad and symmetric. All these characteristics together with the Arrhenius-like temperature dependence of its relaxation times are typical features of secondary relaxations in glass-forming systems and they were also observed in previous works on confined water dynamics.<sup>54–56</sup>

Let us now focus on process 2. The activation energy corresponding to this process is on average 0.38 eV (see Table I). This energy value is similar to that found for water in several hydrophilic solutions at low hydration level and

for water in the first hydration shell of protein–water systems. Moreover, this energy value is lower than that associated with the dielectric reorientation of water molecules having a large mean number of hydrogen bonds (0.54 eV).<sup>41</sup> Therefore, water molecules in C-S-H gel contributing to process 2 at this low hydration level are not involved in a network with a high number of hydrogen bonds per water molecule. Instead, these water molecules establish a small number of hydrogen bonds with the hydrophilic groups at the surface of the C-S-H gel. It is worth mentioning that a dielectric spectroscopy study of an elastomer filled with silica particles with low Si(OH) content reported that one of the relaxation processes (called SP1 in Ref. 57) is due to adsorbed water forming hydrogen bonds with the silanol groups in the surface of the particles. This process is quantitatively similar to our process 2 for the sample CSH-06.

Now we will concentrate on process 3. This process is significantly slower than process 2 and therefore it arises from the reorientation of a different population of water molecules. Its activation energy (roughly 0.52 eV, see Table I) corresponds with that of water molecules involved in the breaking of more than one hydrogen bond. However, the dynamical response is still Arrhenius and therefore the water molecules are not involved in cooperative motions. Therefore a scenario where water molecules responsible for process 3 are connected by more than single hydrogen bond (i.e., water molecules form small clusters) is consistent with our results.

Summarizing, at  $c_w < 10$  wt. % two populations of water molecules are present in the samples. Process 2 is compatible with “bounded” water molecules, whereas process 3 is compatible with “small clusters” of water molecules.

## B. Water dynamics at high hydration level ( $c_w > 10$ wt. %)

Now we focus on the water dynamics of samples with water content higher than 10 wt. %. At this hydration level, profound dynamical changes are observed in both processes 2 and 3 with respect to the low hydration level.

First of all we focus on process 2. In contrast with the results at low water content, the temperature dependence of its relaxation time at  $c_w = 11$  wt. % shows a departure from the Arrhenius behavior at about  $(140 \pm 5)$  K [see Fig. 5(c)]. At the highest water concentration investigated a clear crossover is observed at  $T = 145$  K [see Fig. 5(d)]. The change in the behavior of the relaxation times around 145 K can be well accounted by describing the high-temperature data using a Vogel–Fulcher–Tamman equation<sup>58</sup> (VFT)  $\tau_\omega = \tau_0 \exp(D T_0 / T - T_0)$  with the following parameters:  $\tau_0 = -11.03$  s,  $T_0 = 95.9$  K, and  $D = 10.6$  [see Fig. 5(d)].

In previous works, some of us interpreted the existence of such crossover from high temperature VFT to low-temperature Arrhenius with confinement effects.<sup>41,43,48</sup> Similar finite size effects on the dynamical behavior of the fast component of miscible polymer blends, low molecular weight glass formers/polymers blends or low molecular weight glass formers in soft confinements,<sup>59–61</sup> are usually observed for confinement size ( $d$ ) of  $d = 1–3$  nm. In particular for water molecules, confinement effects were previously observed

for water in graphite oxide<sup>43</sup> ( $d < 1$  nm), water in molecular sieves<sup>62</sup> ( $d = 1$  nm) and water in MCM-41 (Ref. 32) ( $d \approx 1–3$  nm) as well as in molecular dynamics simulations of water in hydrophilic silica surfaces<sup>63</sup> where confinement dependent profiles for the dynamical properties were observed at  $d < 0.6$  nm. In the framework of these ideas, water molecules responsible for process 2 are likely located in small gel pores and therefore finite size effects on its dynamical behavior can be noticed.

In order to define a maximum value of the pore size where water molecules are confined in C-S-H gel, we can obtain some extra information from atomistic simulation for water on the surface of tobermorite.<sup>64</sup> In this case, the size of a water monolayer on a single surface is roughly 0.3 nm. Taking into account that a pore has to be considered as two single surfaces and that as long as we exceed the water content of a monolayer (at 10 wt. %) we observe crossover effects on the dynamical response, the size of our pores should be about 1 nm. In agreement with this observation, atomistic simulations on C-S-H gel by Dolado *et al.*<sup>65</sup> have shown that the width of water layer at 15 wt. % is  $\sim 0.35$  nm. Therefore we can conclude that the size of the pore with water contributing to process 2 should be about 1 nm.

As mentioned above, the appearance of the crossover on the water dynamics at 145 K, takes place at the same water concentration as the formation of one water monolayer on the pore walls.<sup>52</sup> Therefore we can conclude that more than one monolayer of water is a necessary condition for the observation of a crossover in the temperature dependence of the relaxation times corresponding to process 2. Interestingly, in previous studies of water on rutile (TiO<sub>2</sub> nanoparticles) from quasielastic neutron scattering (QENS) experiments and molecular dynamic simulations, Mamontov and co-workers<sup>66</sup> have observed the absence of a crossover below one monolayer covering the particle surface. Note that the water relaxation observed in these systems is qualitatively similar to the process 2 showed in this work.

Now we turn to process 3. This process also evidences a change in the temperature dependence at a threshold of 10 wt. % from an Arrhenius behavior (at low water content) to non-Arrhenius behavior on the whole temperature range (at high water content). However, no crossover on the  $T$ -dependence of the relaxation time was observed at fixed water content. Instead, the  $T$ -dependence of the relaxation times corresponding to process 3 at the highest hydration level [Fig. 5(d)] has a non-Arrhenius behavior which can be fitted with a single VFT equation<sup>58</sup> on the entire temperature range, giving  $\tau_0 = -11.7$ ,  $T_0 = 70$  K, and  $D = 42$ . Note that the VFT parameters are significantly different from those obtained for process 2. From  $D$  and  $T_0$ , a value of the fragility parameter  $m = 25$  is obtained. The fact that the  $T$ -dependence of the relaxation times follows VFT temperature dependence is typical of glass-forming systems and of supercooled liquids of cooperative nature. In other words, as soon as more than one monolayer is detected, water molecules are able to perform cooperative motions as observed in the dielectric response. The obtained value for the fragility parameter,  $m$ , suggests that water involved in process 3 behaves as a relatively strong glass former<sup>67</sup> in this temperature range.

Nevertheless, despite the non-Arrhenius behavior of this process, we have to mention that no calorimetric signature of a corresponding glass transition was observed by DSC. However, we cannot decide whether there is no glass transition related to this process or if the quantity of water molecules involved is not enough to observe such a process by conventional DSC. Finally, we wonder about the absence of a crossover in process 3. In the framework of the idea of confinement effects, water molecules responsible for process 3 should be located in pores large enough to avoid finite size effects. From the previous discussion, these small water clusters could be located in relatively large pores.

Summarizing, we can conclude that each process (2 and 3) represents the relaxation of water molecules localized in different pores of the samples. We attribute the slowest relaxation (process 3) to the collective behavior of clusters of water molecules inside the relatively large pores whereas process 2 is attributed to water in the small pores (<1 nm). This view is in agreement with the work of Ridi *et al.*<sup>40</sup> and Snyder and Bentz,<sup>68</sup> where two populations of water molecules were also estimated from the crystallization detected by means of DSC in highly hydrated cement based materials.

### C. Relation of the dielectric relaxation processes with the cement structure

In this section, we will center the discussion on those aspects related to the cement structure and the state of hydration water. As a starting point, two important and rather established facts should be mentioned: (i) the nanostructure of hydrated cement pastes comprises small (<3 nm) and medium (~10 nm) size pores where water can be located,<sup>52</sup> and (ii) a monolayer of water completely cover the cement paste surface at a relative humidity of 11% (approximately 10 wt. %).

Information on the dynamic properties of water confined in C-S-H gel has been obtained with broadband dielectric spectroscopy in the temperature interval 110–250 K. We were able to distinguish three different relaxation processes related to water in 39 day hydrated C3S samples. In the following, the characteristics of these relaxations will be separately addressed.

The temperature and water concentration dependence of process 2 gives important information about the nature and location of this type of water in hydrated C-S-H. The presence of confinement effects (manifested as a crossover in the temperature dependence of the relaxation times) at high water concentrations indicates that as long as different water molecules start to accumulate, they “feel” the presence of a boundary constraint. This implies that water responsible for process 2 is located in pores of nanoscopic scale and considering previous studies on confined water, confinement sizes should be on the order of few nanometers. Moreover, taking into account that the crossover behavior sets up for water concentrations above that of a monolayer<sup>64,65</sup> and that a monolayer of water is roughly 0.35 nm, water producing process 2 must be confined in small pores of less than 1 nm. Due to this small confining length, this type of water in the context of

the Jennings model<sup>5</sup> would be compatible with interlayer and interglobular (IGP) water.

Regarding water responsible for process 3, it does not present any confinement effect, indicating that for this type of water no topological constraints exist. In this sense, process 3 is compatible with water in larger pores. It is worth noting, however, that at low hydration levels where size effects do not play a role, processes 2 and 3 still show differentiated characteristics and dynamical behavior, evidencing the intrinsic distinct nature of the bonding of these two types of water regardless of the hydration degree. From the values of the activation energies for processes 2 and 3, it turns out that water molecules in process 3 establish a relatively larger number of hydrogen bonds with other water molecules (likely forming small clusters).

Finally, let us comment on process 1. The dielectric strength (intensity) of this process also depends on the water concentration, but this dependence is much weaker than that in processes 2 or 3. This is an indication that process 1 is partially related to water or at least influenced by the presence of water molecules around. In addition, and contrary to the other two processes, process 1 does not disappear after heating the sample at 120 °C. This means that either process 1 comes from the rotation of some intrinsic dipolar group in the C-S-H gel, or from water nonevaporable at 120 °C. The ability of water to avoid evaporation after heating the sample at temperatures over 105 °C has sometimes been used in the literature as a criterion to define “chemical water.” Under this criterion, chemical water could be responsible for the observed dielectric process 1. However, from only dielectric data it is not possible to unambiguously assign the origin of this process to either intrinsic C-S-H dipoles or chemically bound water.

On the other hand, the comparison of the isothermal water adsorption curves of cement pastes and the dielectric and calorimetric behavior of the hydrated C-S-H gel is very motivating. Figure 7 reproduces the first drying measured by

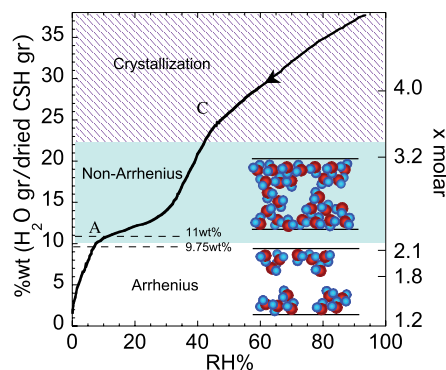


FIG. 7. First drying (thick solid line) curve for  $w/c = 0.5$  cement paste adapted by Jennings from measurements of Powers and Brownard (Ref. 18). The second ordinate represents water content in moles,  $C_{1,7}\text{-S-H}_y$ . Dashed, shadowed, and transparent backgrounds represent crystallization, non-Arrhenius, and Arrhenius regions for water dynamics, respectively. The cartoon represents the location of water molecules corresponding to process 3 (at low hydration level water molecules form small clusters but still show an Arrhenius temperature dependence of the relaxation times, whereas at high hydration level these clusters continue increasing until a VFT behavior typical of cooperative motions is observed).

Powers and Brownyard<sup>8</sup> adapted by Jennings.<sup>5</sup> The left side ordinate represents water content percentage in mass and the right ordinate represents water content in moles, i.e.,  $y$  in  $C_{1.7}\text{-S-H}_y$ .<sup>69</sup> We note that different hydration levels in this work were obtained by drying samples with initial water content of 28 wt. %, therefore “hydration history” should be best described by the first drying curve. One of our main results in this work is that water dynamics is different at low and high hydration levels, showing a deep change at a threshold of 10 wt. %. As discussed in previous sections, from this hydration level, water dynamics is not Arrhenius-like anymore, reflecting the onset of more cooperative-type motions. This change in the dynamics of water from local-type to cooperative-type at 10 wt. % correlates with the reported completion of a water monolayer at around 11% RH (relative humidity) (see point A in Fig. 7), and therefore constitutes an independent and complementary argument for the monolayer formation in the small pores. At higher RH, the thickness of the film adsorbed on the pore walls should increase (i.e., multilayer arrangement) so that water should progressively fill the small pores. Contrary to process 2, water molecules involved in process 3 evidence the formation of small clusters even in the lower hydration levels. This suggests that in the larger pores, water never forms one monolayer but instead small clusters of water would decorate the surface even at low water content (see cartoon in Fig. 7). When hydration increases, these clusters become large enough to evidence cooperative dynamics.

The calorimetric measurements of samples with water content  $\geq 17$  wt. % (not shown in this paper) reveal an exothermic peak upon cooling evidencing the presence of crystallized water. It is well known that the crystallization temperature ( $T_{\text{crys}}$ ) of water decreases when the size of the water reservoir is severely decreased. The  $T_{\text{crys}}$  observed for all the samples with water content  $\geq 17$  wt. % is 227 K, well below the homogeneous nucleation temperature for bulk water (235 K). This fact evidences that after 39 days water in C-S-H gel forms very small water pools so that the presence of “bulk” water can be excluded. Finally, we note that the onset of crystallization correlates quite well with the third change of slope in the first dehydration curve (point C in Fig. 7).

## V. CONCLUSIONS

We have studied the influence of the hydration level on the dielectric response of C-S-H gel. The dielectric spectra revealed three different relaxation processes related to water in 39 day hydrated C3S samples. Each process has shown its own dynamical characteristics and two of them (2 and 3) clearly originated in different populations of water molecules.

Process 2 showed Arrhenius behaviour at low hydration level with relatively low activation energy but as soon as one monolayer of water was reached by increasing hydration, a crossover in the temperature dependence of the relaxation times (from high-temperature non-Arrhenius to low- $T$  Arrhenius) was observed. The presence of this crossover was related with confinement effects and the confinement size was estimated to be 1 nm. On the other hand, process 3 at low

hydration level also showed an Arrhenius behavior but the activation energy was higher than that of process 2, indicating that water clusters exist from low hydration levels. This point questioned the formation of one monolayer in the entire sample. In addition, by increasing the hydration, the probability of water molecules to form big clusters increases and therefore water molecules can relax in a cooperative way. At the higher hydration level (15 wt. %) water dynamics follows a VFT behavior indicative of cooperative-type motions. No confinement effects were observed for this process, indicating that for this type of water no topological constraints exist and therefore water molecules should be located in big pores.

Finally, we have qualitatively related the water dynamics herein observed by BDS with the isothermal water adsorption behavior of cement pastes in the literature.

## ACKNOWLEDGMENTS

Authors gratefully acknowledge the support of Consolider (CSD2006-00053) and Etortek program. S.C. gratefully acknowledge the support of CSIC (200860I021) and S.C. S.A-I, A.A and J.C. gratefully acknowledge the support of the DYNACOP program and the Basque Government, and project IT-436-07 and the Spanish Ministry of Education, and project MAT-22007-63681.

- <sup>1</sup>F. Sanchez and K. Sobolev, *Construct Building mater.* **24**, 2060 (2010).
- <sup>2</sup>K. L. Scrivener and R. J. Kirkpatrick, *Cem. Concr. Res.* **38**, 128 (2008).
- <sup>3</sup>H. F. Taylor, *J. Am. Ceram. Soc.* **69**, 464 (1986).
- <sup>4</sup>H. F. Taylor, *Cement Chemistry*, Academic, New York (1990).
- <sup>5</sup>A. J. Allen, J. J. Thomas, and H. Jennings, *Nat. Mater.* **6**, 311 (2007).
- <sup>6</sup>H. J. H. Brouwers, *Cem. Concr. Res.* **34**, 1697 (2004).
- <sup>7</sup>T. C. Powers, *J. Am. Ceram. Soc.* **41**, 1 (1958).
- <sup>8</sup>T. C. Powers and T. L. Brownyard, *J. Am. Concr. Inst.* **43**, 101 (1947); **43**, 249 (1947); **43**, 469 (1947); **43**, 669 (1947); **43**, 845 (1947); **43**, 865 (1947); **43**, 933 (1947); **43**, 971 (1947).
- <sup>9</sup>R. F. Feldman and P. J. Sereda, *Eng. J. Canada* **53**, 53 (1970).
- <sup>10</sup>P. J. Sereda, R. F. Feldman, and V. S. Ramachandran, *Proceedings of the Seventh International Congress on Chemistry of Cement VI-1/3-VI-1/4* (1980).
- <sup>11</sup>Y. Maréchal, *The Hydrogen Bond and the Water Molecule*, Elsevier, Amsterdam (2007)
- <sup>12</sup>H. M. Jennings, *Cem. Concr. Res.* **30**, 101 (2000).
- <sup>13</sup>H. M. Jennings, *Cem. Concr. Res.* **38**, 275 (2008).
- <sup>14</sup>I. G. Richardson and G. W. Groves, *Cem. Concr. Res.* **22**, 1001 (1992).
- <sup>15</sup>X. Cong and R. J. Kirkpatrick, *Adv. Cem. Based Mater.* **3**, 144 (1996).
- <sup>16</sup>A. Nonat and X. Lecoq, in *Nuclear Magnetic Resonance Spectroscopy of Cement-Based Materials*, edited by P. Colombet, A. R. Gmitter, H. Zanni, and P. Sozzani, Springer, Berlin (1998), pp. 197–207.
- <sup>17</sup>J. J. Chen, J. T. Thomas, H. F. Taylor, and H. M. Jennings, *Cem. Concr. Res.* **34**, 1499 (2004).
- <sup>18</sup>I. G. Richardson, *Cem. Concr. Res.* **34**, 1733 (2004).
- <sup>19</sup>J. S. Dolado, J. Hamaekers, and M. Griebel, *J. Am. Ceram. Soc.* **90**, 3938 (2007).
- <sup>20</sup>L. B. Skinner S. R. Chae, C. J. Benmore, H. R. Wenk, and P. J. M. Monteiro, *Phys. Rev. Lett.* **104**, 195502 (2010).
- <sup>21</sup>A. J. Bohris, U. Goerke, P. J. McDonald, M. Mulheron, B. Newling, and B. Le Page, *Magn. Reson. Imaging* **16**, 455 (1998).
- <sup>22</sup>J. P. Korb, P. J. McDonald, L. Monteilhet, A. G. Kalinichev, and R. J. Kirkpatrick, *Cem. Concr. Res.* **37**, 348 (2007).
- <sup>23</sup>J.P. Korb, *Curr. Opin. in Collo. Interface Sci.* **14**, 192 (2009).
- <sup>24</sup>R. Berliner, M. Popovici, K. W. Herwig, M. Berliner, H. M. Jennings, and J. J. Thomas, *Cem. Concr. Res.* **28**, 231 (1998).
- <sup>25</sup>V. K. Peterson, D. A. Neumann, and R. A. Livingston. *J. Phys. Chem. B* **109**, 14449 (2005).

- <sup>26</sup>H. N. Bordallo, L. P. Aldridge, and A. Desmedt, *J. Phys. Chem. B* **110**, 17966 (2006).
- <sup>27</sup>N. E. Hager and R. C. Domszy, *J. Appl. Phys.* **96**, 5117 (2004).
- <sup>28</sup>N. Miura, N. Shinyashiki, S. Yagihara, and M. Shiotsubo, *J. Am. Ceram. Soc.* **81**, 213 (1998).
- <sup>29</sup>S. Yagihara *et al.*, *Subsurface Sensing Technologies Applications* **2**, 15 (2001).
- <sup>30</sup>L. Hanzic, G. Mandzuka, and D. Korosak, on *Innovations in Structural Engineering and Construction, Proceedings and Monographs in Engineering, Water and Earth Sciences*, edited by Y. M. Xie and I. Patnaikuni, p. 501 (2008).
- <sup>31</sup>C. Tsonos, I. Stavrakas, C. Anastasiadis, A. Kyruazopoulos, A. Kanapitsas, and D. Triantis, *J. Phys. Chem. Solids* **70**, 576 (2009).
- <sup>32</sup>J. Sjostrom, J. Swenson, R. Bergman, and S. Kittaka, *J. Chem. Phys.* **128**, 154503 (2008); K. Yoshida, T. Yamaguchi, S. Kittaka, M. C. Bellissent-Funel, and P. Fouquet, *J. Chem. Phys.* **129**, 054702 (2008).
- <sup>33</sup>L. Liu *et al.*, *Phys. Rev. Lett.* **95**, 117802 (2005); J. Swenson, *Phys. Rev. Lett.* **97**, 189901 (2006); S. Cerveny, A. Alegria, and J. Colmenero, *Phys. Rev. Lett.* **97**, 189802 (2006).
- <sup>34</sup>W. Doster, S. Busch, A. M. Gaspar, M. S. Appavou, J. Wuttke, and H. Scheer, *Phys. Rev. Lett.* **104**, 098101 (2010); S. H. Chen *et al.*, *Proc. Natl. Acad. Sci. USA* **103**, 9012 (2006).
- <sup>35</sup>M. Vogel, *Phys. Rev. Lett.* **101**, 225701 (2008).
- <sup>36</sup>F. Kremer and A. Schönhal, *Broadband Dielectric Spectroscopy*, Springer Berlin (2003).
- <sup>37</sup>U. Kaatz and Y. Feldman, *Meas. Sci. Technol.* **17**, R17 (2006).
- <sup>38</sup>N. Nandi, K. Bhattacharyya, and B. Bagchi, *Chem. Rev.* **100**, 2013 (2000).
- <sup>39</sup>R. H. Cole and K. S. Cole, *J. Chem. Phys.* **10**, 98 (1942).
- <sup>40</sup>F. Ridi, P. Luciani, E. Frantini, and P. Baglioni, *J. Phys. Chem B* **113**, 3080 (2009).
- <sup>41</sup>S. Cerveny, A. Alegria, and J. Colmenero, *Phys. Rev. E* **77**, 031801 (2008).
- <sup>42</sup>C. Gainaru, A. Fillmer, and R. Böhmer, *J. Phys. Chem. B* **113**, 12628 (2009).
- <sup>43</sup>S. Cerveny, F. Barroso-Bujans, A. Alegria, and J. Colmenero, *J. Phys. Chem. C* **114**, 2604 (2010).
- <sup>44</sup>J. Swenson, H. Jansson, H. Hedstroem, and R. Bergman, *J. Phys. Condens. Matter* **19**, 205109 (2007).
- <sup>45</sup>Y. Hayashi, A. Puzenko, I. Balin, Y. E. Ryabov, and J. Feldman, *J. Phys. Chem B* **109**, 9174 (2005).
- <sup>46</sup>H. Jansson, R. Bergman, and J. Swenson, *J. Phys. Chem B* **109**, 24134 (2005).
- <sup>47</sup>L. T. Zhuravlev, *Colloids Surf., A* **173**, 1 (2000).
- <sup>48</sup>S. Cerveny, A. Alegria, and J. Colmenero, *J. Chem. Phys.* **128**, 044901 (2008).
- <sup>49</sup>N. E. Hager III and R. C. Domszy, *J. Appl. Phys.* **96**, 5117 (2004).
- <sup>50</sup>N. Miura, N. Shinyashiki, S. Yagihara, and M. Shiotsubo, *J. Am. Cer. Soc.* **81**, 213 (1998).
- <sup>51</sup>Y. El Hafiane, A. Smith, J. P. Bonnet, P. Abelard, and P. Blanchart, *Cem. Concr. Res.* **30**, 1057 (2000).
- <sup>52</sup>Kalliopi K. Aligizaki., *Modern Concrete Technology Series*; v.12, Taylor & Francis, London (2006).
- <sup>53</sup>S. Cerveny, A. Alegria, and J. Colmenero, *Eu. Phys. J.-Special Topics* **141**, 49 (2007).
- <sup>54</sup>S. Cerveny, G. A. Schwartz, R. Bergman, and J. Swenson, *Phys. Rev. Lett.* **93**, 245702 (2004).
- <sup>55</sup>J. Swenson, H. Jansson, and R. Bergman, *Phys. Rev. Lett.* **96**, 247802 (2006).
- <sup>56</sup>S. Capaccioli, K. L. Ngai, and N. Shinyashiki, *J. Phys. Chem. B* **111**, 8197 (2007); K. L. Ngai, S. Capaccioli, and N. Shinyashiki, *J. Phys. Chem. B* **112**, 3826 (2008).
- <sup>57</sup>J. G. Meier, J. Fritzsche, L. Guy, Y. Bomal, M. Klüppel, *Macromolecules* **42**, 2127 V15GH (2009).
- <sup>58</sup>H. Vogel, *Phys. Z.* **22**, 645 (1921); G. S. Fulcher, *J. Am. Chem. Soc.* **8**, 339 (1925); **8**, 789 (1925).
- <sup>59</sup>G. A. Schwartz, A. Alegria, and J. Colmenero, *J. Chem. Phys.* **127**, 154907 (2007); *Macromolecules* **40**, 3246 (2007).
- <sup>60</sup>D. Cangialosi, A. Alegria, and J. Colmenero, *J. Chem Phys.* **128**, 224508 (2008); *Phys. Rev. E* **80**, 041505 (2009).
- <sup>61</sup>T. Blochowicz, E. Gouirand, A. Fricke, T. Spehr, B. Stühn, and B. Frick, *Chem. Phys. Lett.* **475**, 171 (2009).
- <sup>62</sup>H. Jansson and J. Swenson, *Eur. Phys. J. E* **12**, S51 (2003).
- <sup>63</sup>S. R. V. Castrillon, N. Giovambattista, I. A. Aksay, and P. G. Debenedetti, *J. Phys. Chem B* **113**, 7973 (2009).
- <sup>64</sup>A. G. Kalinichev, *Cem. Concr. Res.* **37**, 3377 (2007).
- <sup>65</sup>J. Dolado *et al.*, "The nano-branched structure of C-S-H gel" *J. Mat. Chem.* submitted to.
- <sup>66</sup>E. Mamontov, L. Viecek, D. J. Wesolowski, P. T. Cummings, J. Rosenqvist, W. Wang, D. R. Cole, L. M. Anovitz, and G. Gasparovic, *Phys. Rev. E* **79**, 51504 (2009).
- <sup>67</sup>C. A. Angell, *J. Phys. Chem.* **97**, 6339 (1993).
- <sup>68</sup>K. A. Snyder and D. P. Bentz, *Cem. Concr. Res.* **34**, 2045 (2004).
- <sup>69</sup>We chose  $y = 1.2$  as a reference for the "dried" state instead of  $y = 1.3$  proposed by Jennings because our samples were oven dried at 100 °C. In any case, the choice of one or the other only changes slightly wt % to  $y$  conversion ( $\Delta\psi \sim 0.1$  in  $y$  units), and does not affect the discussion herein.